

RESEARCH LETTER

Open Access



Potential deployment of offshore bottom pressure gauges and adoption of data assimilation for tsunami warning system in the western Mediterranean Sea

Mohammad Heidarzadeh^{1*}, Yuchen Wang², Kenji Satake² and Iyan E. Mulia²

Abstract

Western Mediterranean Basin (WMB) is among tsunamigenic zones with numerous historical records of tsunami damage and deaths. Most recently, a moderate tsunami on 21 May 2003 offshore Algeria, North Africa, was a fresh call for strengthening tsunami warning capabilities in this enclosed water basin. Here, we propose to deploy offshore bottom pressure gauges (OBPGs) and to adopt the framework of a tsunami data assimilation (TDA) approach for providing timely tsunami forecasts. We demonstrate the potential enhancement of the tsunami warning system through the case study of the 2003 Algeria tsunami. Four scenarios of OBPG arrangements involving 10, 5, 3 and 2 gauges are considered. The offshore gauges are located at distances of 120–300 km from the North African coast. The warning lead times are 20, 30, 48 and 55 min for four points of interest considered in this study: Ibiza, Palma, Sant Antoni and Barcelona, respectively. The forecast accuracies are in the range of 69–85% for the four OBPG scenarios revealing acceptable accuracies for tsunami warnings. We conclude that installation of OBPGs in the WMB can be helpful for providing successful and timely tsunami forecasts. We note that the OBPG scenarios proposed in this study are applicable only for the case of the 2003 Algeria tsunami. Further studies including sensitivity analyses (e.g., number of OBPG stations; earthquake magnitude, strike, epicenter) are required in order to determine OBPG arrangements that could be useful for various earthquake scenarios in the WMB.

Keywords: Mediterranean Sea, Tsunami, Earthquake, Tsunami warning system, Offshore bottom pressure gauge, Tsunami data assimilation

Introduction

Western Mediterranean Basin (WMB) is a tsunamigenic zone within the Mediterranean Sea posing tsunami risks to Italy, France, Spain, Morocco, Algeria and Tunisia (Fig. 1). The region has experienced several tsunamis in the past; most recently on 21 May 2003 when a 2-m tsunami was generated following an Mw 6.9 earthquake offshore Algeria (Fig. 1) (Alasset et al. 2006; Sahal et al. 2009; Heidarzadeh and Satake 2013). The tsunami was

recorded on several tide gauges in the WMB including the four stations of Ibiza, Palma, Sant Antoni and Barcelona (Fig. 1). Other notable tsunamis in the WMB are: the 23 February 1887 event on the Ligurian Coast (Larrouque et al. 2012; Eva and Rabinovich 1997) and the 21 August 1856 Djijelli (Algeria) tsunami (Roger and Hébert 2008) (stars in Fig. 1). Based on historical data of tsunami occurrences in the WMB, Soloviev (1990) identified four tsunamigenic zones in this basin namely: the coast of Spain (CoS), the North African Coast (NAC), the Ligurian Sea (LS) and the west coast of Italy and Tyrrhenian Sea (WCITS) (Fig. 1). Historical earthquake data based on the United States Geological Survey's catalogue ($M > 5$) reveal that these four zones correspond to those

*Correspondence: mohammad.heidarzadeh@brunel.ac.uk

¹ Department of Civil & Environmental Engineering, Brunel University London, Uxbridge UB8 3PH, UK

Full list of author information is available at the end of the article

Author Proof

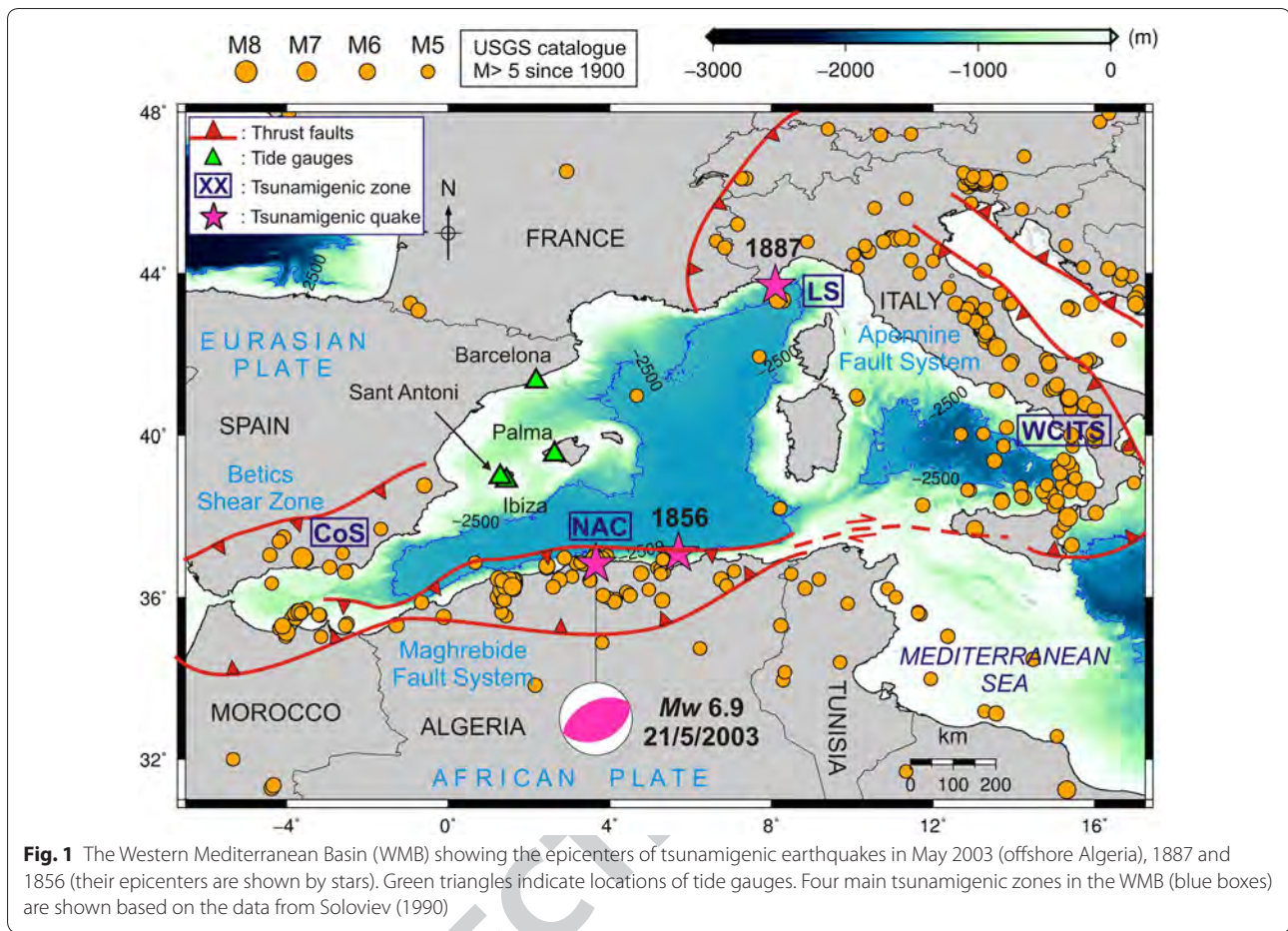


Fig. 1 The Western Mediterranean Basin (WMB) showing the epicenters of tsunamigenic earthquakes in May 2003 (offshore Algeria), 1887 and 1856 (their epicenters are shown by stars). Green triangles indicate locations of tide gauges. Four main tsunamigenic zones in the WMB (blue boxes) are shown based on the data from Soloviev (1990)

47 with highest seismic activities within the WMB, in particular NAC and WCITS. The high seismic activity in this region is the result of the complicated tectonic boundaries between the African and Eurasian plates involving several micro-plates as well as multiple convergent and divergent plate boundaries (Fig. 1).

49 Due to such high seismicity and existing records of tsunami occurrences, tsunami warning systems have been developed for the Mediterranean basin in the framework of the NEAMTWS (North East Atlantic, Mediterranean and Connected seas Tsunami Warning System) since 2005 (Tinti et al. 2012; Papadopoulos and Fokaefs 2013; Papadopoulos 2015; IOC 2015; Necmioglu and Özel 2015; Necmioglu 2016; Okal et al. 2009; Synolakis and Bernard 2006; Satake 2014). Starting from 2017, several countries (i.e., France, Greece, Italy, and Turkey) are equipped with national tsunami warning centers and act as Tsunami Service Providers (TSPs). Some other countries, including Portugal and Spain, will develop such capacities in the near future (Heidarzadeh et al. 2017). The performance of the Mediterranean TSPs has been tested during the 20 July 2017 Bodrum–Kos (Turkey–Greece) Mw 6.6 earthquake and tsunami revealing

satisfactory response by three operational TSPs namely: CAT-INGV (Italy), KOERI-RETMC (Turkey), and NOA/HL-NTWC (Greece) (Heidarzadeh et al. 2017; Dogan et al. 2019; Öztürk and Şahin 2019).

Although the response of the regional TSPs to the July 2017 event was assessed to be satisfactory, that moderate tsunami revealed that more investment should be devoted to the Mediterranean TSPs in two fronts: equipment for monitoring tsunamis and public education. In terms of equipment, Heidarzadeh et al. (2017) specifically pointed out the potential application of offshore tsunami gauges in the Mediterranean Sea. In the aftermath of the giant 2004 Indian Ocean tsunami, tens of offshore bottom pressure gauges (OBPGs) have been installed across the world oceans which are called Deep-Ocean Assessment and Reporting of Tsunamis (DART) (Gonzalez et al. 1998; Synolakis and Bernard 2006; Rabinovich and Eblé 2015; Heidarzadeh et al. 2015, 2016) which are spaced in the range of 400–4000 km from each other (Heidarzadeh and Gusman 2018). Two dense networks of OBPGs, called Seafloor Observation Network for Earthquakes and Tsunamis (S-net) and Dense Ocean-floor Network System for Earthquakes and Tsunamis

(DONET), were deployed by the Japanese Government, with 150 gauges spaced approximately 30–50 km (Kanazawa 2013) for S-net and 51 gauges spaced 15–20 km for DONET (Kaneda et al. 2009, 2015). Such relatively dense offshore observation network provides the opportunity to use the real-time sea level data for tsunami forecast through tsunami data assimilation (TDA) (Maeda et al. 2015; Gusman et al. 2016; Wang et al. 2018). Although the TDA approach requires a relatively expensive network of OBPBs, it greatly improves the accuracy of tsunami forecasts.

The purpose of this study is to investigate whether a network of OBPBs can be effective for tsunami forecast in the WMB through a case study of the May 2003 earthquake and tsunami. Figure 2 provides tsunami travel time (TTT) analyses, using the software by Geoware (2011), for tsunamigenic earthquakes in two zones in the WMB namely the NAC (i.e., the 2003 tsunami in southern WMB) and LS (i.e., the 1887 tsunami in northern WMB) indicating that it takes approximately 70–80 min for the tsunami generated in each of these zones to arrive at the opposite coast in the WMB. Such relatively long TTT may imply that the WMB has the potential for application of TDA approach for tsunami forecast. We propose a hypothetical OBPB network and apply the TDA technique to investigate its effectiveness. A preliminary sensitivity analysis is performed to determine the performance of the system for different number of OBPBs.

The May 2003 Algeria earthquake (Mw 6.9) and tsunami

The 2003 Algeria earthquake was a thrust earthquake, with Mw 6.8–6.9 (Meghraoui et al. 2004; Déverchère et al. 2005) that occurred on 21 May at 18:44 UTC offshore north coast of Algeria (Fig. 3). The earthquake left more than 2000 deaths but the tsunami was moderate and no death was linked to the tsunami whose height was reported to be up to approximately 2 m (Alasset et al. 2006; Sahal et al. 2009). The tsunami waveform data used in this study include four tide gauge records in Ibiza, Palma, Sant Antoni and Barcelona with sampling intervals of 5, 1, 2 and 5 min, respectively (Fig. 2). Detailed information about these tide gauges are presented in Heidarzadeh and Satake (2013). While sampling intervals of 1 and 2 min (Palma and Sant Antoni) relatively well allow recording of the tsunami signals, the sampling interval of 5 min (Ibiza and Barcelona) may not permit the full registration of the tsunami. It may be noted that most tide gauges worldwide were programmed for long sampling intervals of 5–15 min before the 2004 Indian Ocean tsunami. The sea level data used in this study are provided by UNESCO-IOC (Intergovernmental Oceanographic Commission), Puertos del Estado (Spain) (<http://www.puertos.es/>) and the European Sea Level Service.

The tsunami recorded by tide gauges in the region (Fig. 3) show trough-to-crest wave heights of 59, 116, 196 and 43 cm in Ibiza, Palma, Sant Antoni and Barcelona, respectively (Heidarzadeh and Satake 2013). Note that

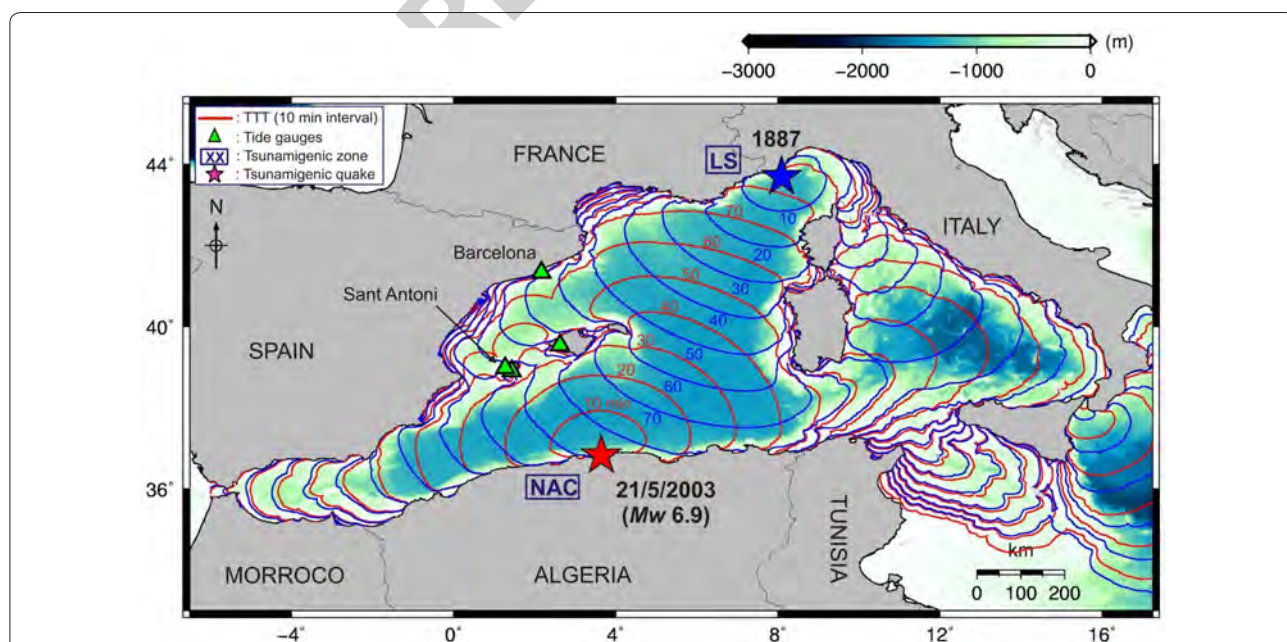


Fig. 2 Tsunami travel time (TTT) analysis for the 21 May 2003 (offshore Algeria) tsunami and the 1887 Ligurian Coast tsunami with contours of 10-min intervals

Author Proof

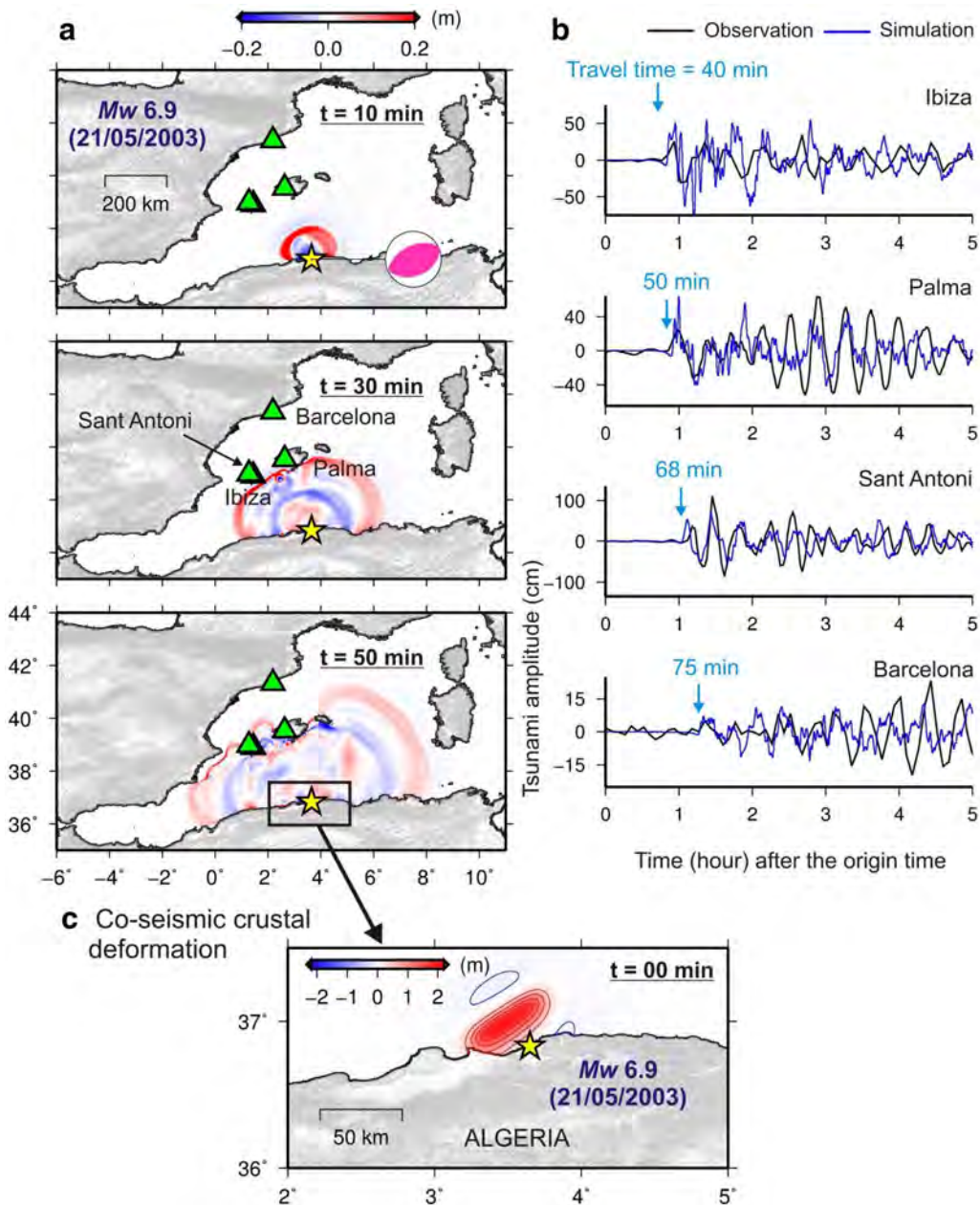


Fig. 3 **a** Tsunami snapshots of the 21 May 2003 (offshore Algeria) tsunami. **b** Observed (black) and simulated (blue) tsunami waveforms at tide gauges. **c** The source model used for simulation which is based on that proposed by Heidarzadeh and Satake (2013). Note that the two stations of Ibiza and Sant Antoni are very close to each other and their symbols are overlapped. Sant Antoni station is located to the west on Ibiza

150 the two stations of Ibiza and Sant Antoni, both in Ibiza
 151 island, are very close to each other and are overlapped
 152 in Fig. 3a; Sant Antoni station is located to the west
 153 on Ibiza. Based on the tide gauge data and TTT analysis,
 154 the tsunami arrived in Balearic Islands (Ibiza, Palma)
 155 after ~40 min, whereas it took 60–75 min for the waves
 156 to arrive at mainland France and Spain (Figs. 2, 3). The
 157 relatively long travel time of up to 75 min for tsunamis

from the NAC zone to the coasts of Spain, France and
 other coasts in the WMB enables the application of TDA
 approach in a real-time tsunami forecast system.

Data and methods

Bathymetry data are based on the 30 arc-sec grid of General Bathymetric Charts of the Oceans (GEBCO, Weatherall et al. 2015) which was interpolated to a 475-m grid

158
 159
 160
 161
 162
 163
 164

165 in this study. Forward tsunami modeling was conducted
 166 applying the Nonlinear Shallow Water tsunami model
 167 TUNAMI-N2 (Goto et al. 1997; Yalçiner et al. 2004)
 168 using a time step of 1.0 s and a total duration of 5 h for
 169 tsunami simulations on a single grid with Cartesian coordi-
 170 nate system. The tsunami source of the May 2003 event
 171 was based on that of Heidarzadeh and Satake (2013) hav-
 172 ing dimensions of 60 km × 30 km and a uniform slip of
 173 2 m. The dislocation model of Okada (1985) was used
 174 to calculate the co-seismic crustal deformation as initial
 175 condition for tsunami propagation modeling. The soft-
 176 ware tsunami travel times (TTT) by Geoware (2011) was
 177 used for tsunami travel time analysis.

178 To examine the performance of OBPGs for tsunami
 179 forecast in the WMB through TDA approach, we con-
 180 sider a case study involving the NAC as the tsunamigenic
 181 zone and the May 2003 tsunami (Fig. 4) as a real tsunami
 182 event. We consider hypothetical OBPGs within the WMB
 183 and then investigate whether a TDA approach can benefit
 184 from them to provide timely tsunami forecasts for coasts of
 185 Spain and France in case a tsunami is generated from the
 186 NAC. Since an OBPG network is usually expensive in terms
 187 of installation and maintenance, it is important to design an
 188 efficient network with minimum number of OBPGs. Here,
 189 we considered four scenarios. The first scenario contains
 190 ten buoys (Fig. 4b) distributed at two rows with buoy spac-
 191 ing intervals of approximately 50 km. The second scenario

192 contains five buoys (Fig. 4c) by removing the northern row
 193 of the first scenario. The third and fourth scenarios contain
 194 three and two buoys, respectively, with spatial intervals of
 195 ~100 km (Fig. 4d, e). The OBPGs in these four scenarios
 196 are distanced approximately 120–300 km from the North
 197 African coast.

198 For TDA, we adopted the optimal interpolation for
 199 tsunami data assimilation, because it has a relatively
 200 smaller computational cost than the ensemble Kalman
 201 filter (Maeda et al. 2015; Yang et al. 2019). This algo-
 202 rithm reconstructs the tsunami wavefield from the data
 203 of offshore tsunami observations through minimiz-
 204 ing the total error of all the observations (Kalnay 2003).
 205 In the numerical simulation, we represent the tsunami
 206 wavefield at the n th time step as the vector \mathbf{x}_n defined as:
 207 $\mathbf{x}_n = (h(n\Delta t, x, y), M(n\Delta t, x, y), N(n\Delta t, x, y))$, where
 208 h is the tsunami height, M and N are depth-integrated
 209 flow discharge fluxes in two horizontal directions of x
 210 and y . The offshore pressure gauges directly provide data
 211 of tsunami height, but the velocity components of \mathbf{x}_n are
 212 reconstructed during the assimilation process. The TDA
 213 approach is described by the following two equations
 214 (Maeda et al. 2015):

$$\mathbf{x}_n^f = F\mathbf{x}_{n-1}^a, \tag{1}$$

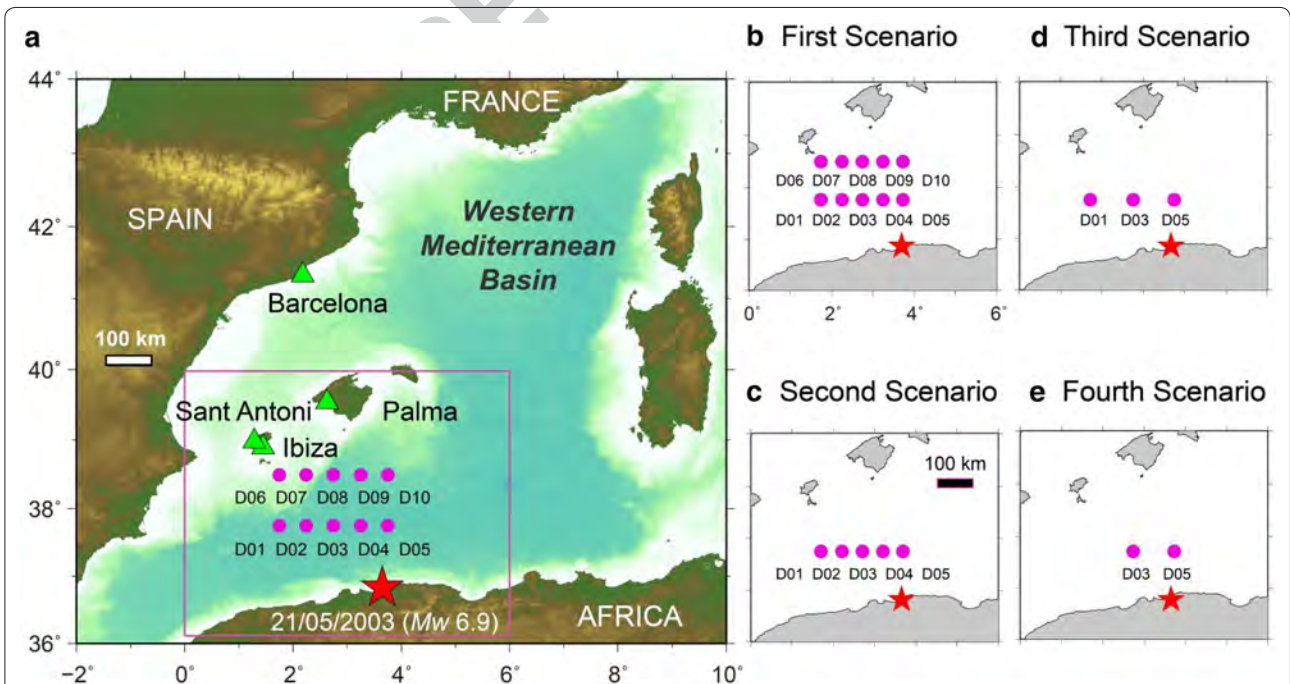


Fig. 4 Different tsunami data assimilation scenarios employing 10, 5, 3 and 2 offshore tsunami pressure gauges (pink solid circles). Triangles and the star show the locations of tide gauges and the May 2003 epicenter, respectively

Author Proof

$$\mathbf{x}_n^a = \mathbf{x}_n^f + \mathbf{W}(\mathbf{y}_n - \mathbf{H}\mathbf{x}_n^f). \tag{2}$$

By using Eq. (1), we calculate the forecasted tsunami wavefield \mathbf{x}_n^f in time step n from the assimilated tsunami wavefield at the previous time step \mathbf{x}_{n-1}^a . The matrix \mathbf{F} is called the propagation matrix which corresponds to the tsunami propagation model. In Eq. (2), we assimilate the observed data in order to correct the forecasted tsunami wavefield. The observation matrix \mathbf{H} is a sparse matrix, which contains only 0 and 1 values. It extracts the tsunami height from the forecasted wavefield, and calculates the residual with the real-time observed tsunami heights \mathbf{y}_n . Consequently, the residual is multiplied by the weight matrix \mathbf{W} to bring the assimilated wavefield closer to the real observation (Maeda et al. 2015; Gusman et al. 2016). To minimize the total error, we compute the weight matrix by solving the following linear system:

$$\mathbf{W}(\mathbf{R} + \mathbf{H}\mathbf{P}^f\mathbf{H}^T) = \mathbf{P}^f\mathbf{H}^T, \tag{3}$$

where $\mathbf{P}^f = \langle \varepsilon^f \varepsilon^{fT} \rangle$ and $\mathbf{R} = \langle \varepsilon^O \varepsilon^{OT} \rangle$ are the covariance matrices of the forward numerical simulation and the observations, respectively. ε^f and ε^O are the Gaussian errors associated with forward numerical simulations and observations, respectively, and ε^{fT} and ε^{OT} are the corresponding transpose matrixes. We assume that the computational errors are spatially homogeneous on numerical grids, and the observation errors are uncorrelated among stations because observations are made independently. These assumptions simplified the matrix \mathbf{R} into a diagonal matrix whose diagonal component was the standard deviation of the observation error at each station (Maeda et al. 2015). For both matrices, we assume a Gaussian-distributed covariance, with a characteristic distance of 20 km (Maeda et al. 2015; Wang et al. 2018). By repeatedly solving Eqs. (1) and (2) consequently, the tsunami wavefield is gradually assimilated, and the forecasted waveforms at any location inside the model domain can be obtained.

To evaluate the performance of the forecast, we selected four points of interest (PoIs) where actual tsunami observations from the May 2003 tsunami are available (i.e., Barcelona, Sant Antoni, Ibiza and Palma; Fig. 4a) and are used for waveform comparisons. We defined the time period during which the observational data are used for assimilation as the time window (Wang et al. 2017). A longer time window indicates that the tsunami passes through more OBPBs, and thus longer waveform data are assimilated. In this study, a time window of 20 min, starting from the earthquake origin time, was used for TDA (Fig. 5a). The waveforms in Fig. 5a are the results of forward simulations of the 2003 tsunami using the source model shown in Fig. 3c. As tsunami travel time

from the source of the May 2003 tsunami to the nearest OBPB is approximately 7 min (Fig. 3), the time window of 20 min implies that 13 min of tsunami signals recorded on OBPBs will be used for assimilation. The time available to giving tsunami warnings to coastal areas, called as warning lead time, is the time interval between the end of the TDA and the tsunami arrival time (Fig. 5b).

The forecasted tsunami waveforms by the TDA are compared with simulated waveforms and observations at the PoIs. Both simulated and actual observation waveforms were used for forecast accuracy analysis in this study. To quantitatively analyze the accuracy of the forecasts, we applied a method for waveform comparisons by considering both the first-peak amplitude and the maximum amplitude of the tsunami, similar to the score of Tsushima et al. (2009) and the index of VRO of Yamamoto et al. (2016). Our method for waveform comparison applies the following equation:

$$K = 1 - \frac{\sum (H_f^{\max} - H_o^{\max})^2 + \sum (H_f^{\text{arr}} - H_o^{\text{arr}})^2}{\sum (H_o^{\max})^2 + \sum (H_o^{\text{arr}})^2}, \tag{4}$$

where N is the number of PoIs, the subscripts f and o represent the forecasted and observed tsunami waveforms, respectively. H^{\max} is the maximum amplitude of the tsunami, and H^{arr} is the first-peak amplitude. A K value closer to 1 indicates a better forecast. We multiplied the results of Eq. (4) with 100 to obtain percentage of forecast accuracy.

Results and discussion

Results of TDA for the May 2003 tsunami are given in Figs. 6 and 7 for the scenarios of 10, 5, 3 and 2 OBPBs. The forecast accuracy analysis is based on the comparison of the TDA-forecasted waveforms with observation (blue columns in Fig. 8) and simulations (orange columns in Fig. 8). It can be seen that the assimilated waveforms (red) match fairly well with the first tsunami cycle of the observations (black) in all four scenarios. Although the agreement is generally well in terms of wave period, the assimilated waveform in Sant Antoni arrives ~10 min earlier than the observation. We attribute this travel time difference to the location of the Sant Antoni tide gauge station, which is inside the semi-enclosed bay with irregular coastal geometry and shallow bathymetry that significantly affect the tsunami travel time. A high-resolution bathymetry with a spatial resolution of at least 50 m is required to more accurately model the tsunami travel time to Sant Antoni. We also note that the relatively smooth waveforms of the observations is due to the low sampling rates of 5 and 2 min while our simulations and assimilations possess temporal intervals of 1 s. The third

Author Proof

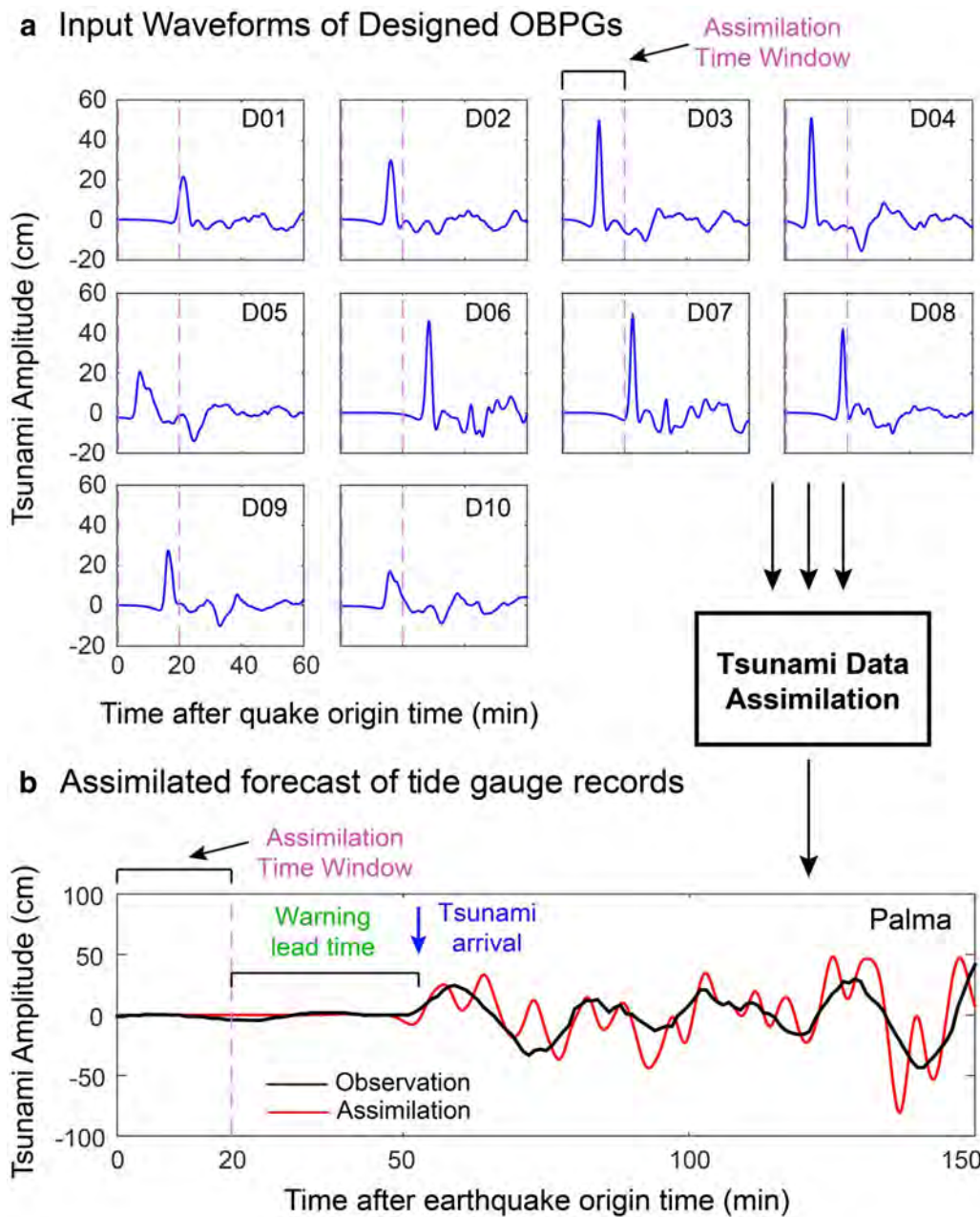


Fig. 5 Tsunami data assimilation process employing 20-min tsunami observation data from the OBPGs (a) and the forecasted tsunami in Palma using the tsunami data assimilation method (b)

318 and fourth scenarios (3 and 2 OBPGs) appear to under-
 319 estimate the first and second large peaks in Sant Antoni
 320 although they give acceptable estimations in other three
 321 PoIs.

322 Figure 8 presents the overall forecast accuracy for each
 323 of the four TDA scenarios by comparing the assimilated
 324 waveforms with both observations and simulations. The
 325 comparison with simulations gives better accuracies than

with observations; we discuss here the forecast accuracies
 based on the comparison of the assimilated and observed
 waveforms. As expected, the first and the fourth scenarios
 yield the best and the worst performances, with forecast
 accuracies of 85% and 69%, respectively. Since we used a
 time window of 20 min for assimilation and given the TTTs
 shown in Figs. 2, 3, the tsunami warning lead times for
 Ibiza, Palma, Sant Antoni and Barcelona

326
 327
 328
 329
 330
 331
 332
 333

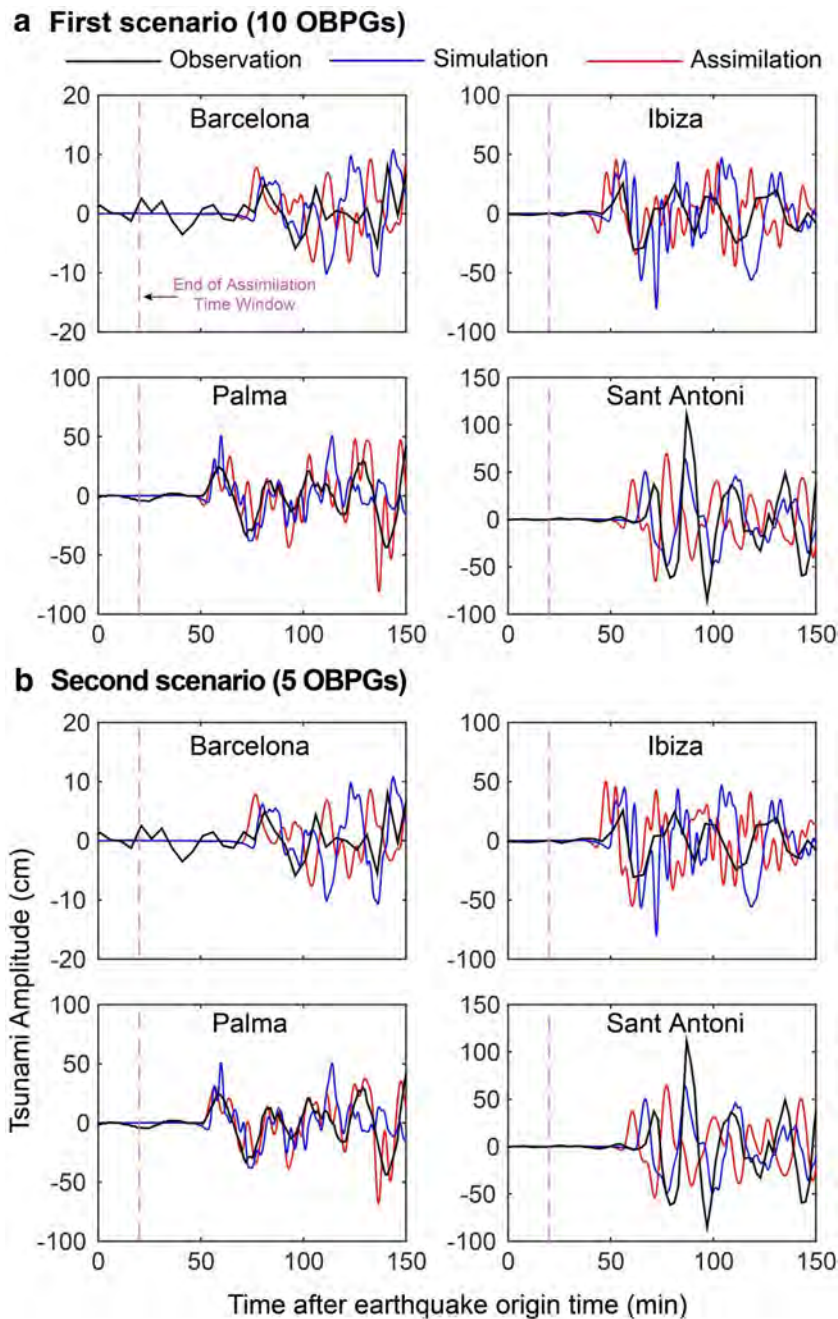


Fig. 6 Comparison of the observations (black lines), simulation (blue lines) and forecasted (data assimilation; red lines) waveforms at four PoIs for the first (a; 10 OBPGs) and second (b; five OBPGs) scenarios. The time window for assimilation is 20 min (dashed vertical line)

334 are 20, 30, 48 and 55 min, respectively. These lead times
 335 are sufficient to allow for effective tsunami warnings in
 336 all of these PoIs. We conclude that all of the four OBPG
 337 scenarios result in satisfactory performances towards
 338 forecasting the May 2003 tsunami. This indicates that
 339 deployment of OBPGs is beneficial for the tsunami warn-
 340 ing system in the WMB.

The success of all four scenarios involving 2–10 OBPGs
 in forecasting of the May 2003 tsunami could be attrib-
 uted to the relatively small size of the tsunami source
 (~70 km; Fig. 3c), the SW–NE strike of the tsunami-
 genic fault (Fig. 3c), as well as the short distances of the
 OBPGs to the tsunami source area. The two OBPGs in
 scenario 4 can efficiently capture most of the May 2003

341
 342
 343
 344
 345
 346
 347

Author Proof

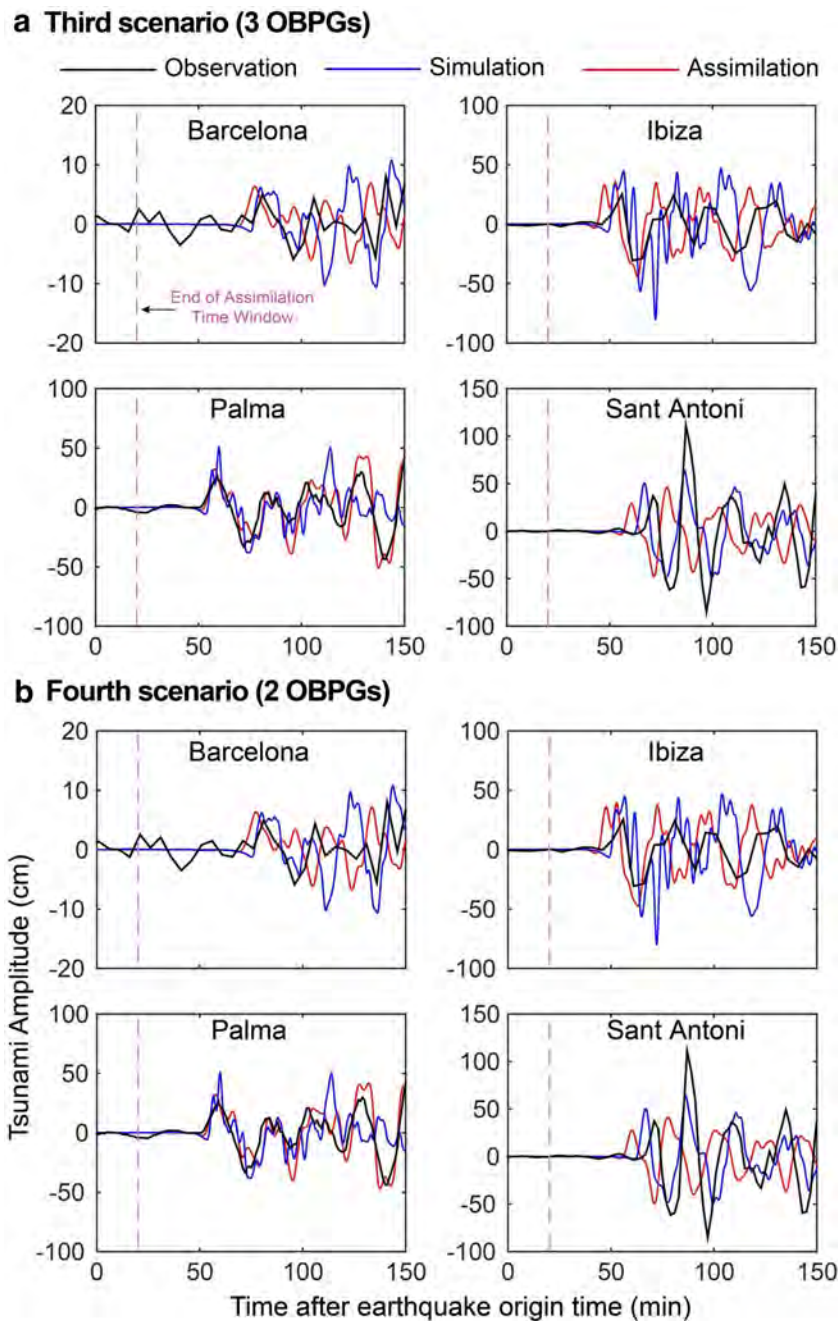


Fig. 7 Comparison of the observations (black lines), simulation (blue lines) and forecasted (data assimilation; red lines) waveforms at four Pols for the third (**a**; three OBPGs) and fourth (**b**; two OBPGs) scenarios. The time window for assimilation is 20 min (dashed vertical line)

348 tsunami characteristics because they are spaced 100 km
 349 from each other, are aligned E–W and are located at the
 350 distance of 120–170 km from the epicenter. However,
 351 this result may not indicate that the scenario 4 (involving
 352 two OBPGs) will give the same forecast accuracy for
 353 other tsunamis with different sizes and strike angles. Our
 354 experience (Wang et al. 2019) showed that the larger

the tsunami size and wavelength, the more OBPGs is
 required for accurate TDA. Clearly, detailed sensitivity
 analyses considering various earthquake scenarios
 (magnitude, strike, epicenter) combined with numerous
 OBPGs arrangements (number, alignment, spacing)
 (Mulia et al. 2017, 2019) are necessary to determine the
 optimum OBPGs network design for the WMB which

355
 356
 357
 358
 359
 360
 361

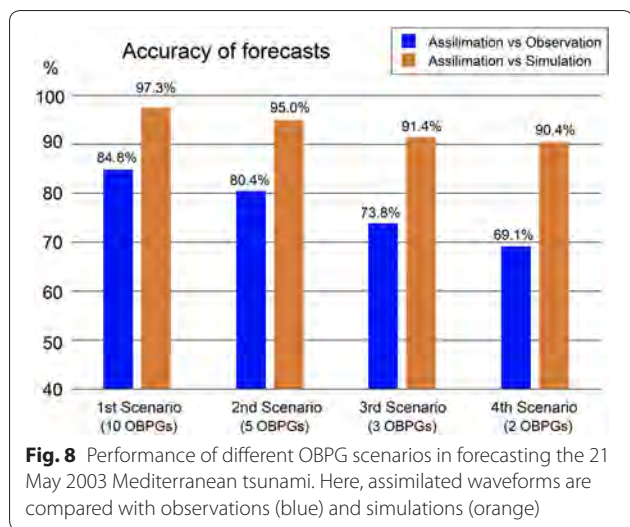


Fig. 8 Performance of different OBPG scenarios in forecasting the 21 May 2003 Mediterranean tsunami. Here, assimilated waveforms are compared with observations (blue) and simulations (orange)

can address tsunami threats from all four tsunamigenic zones in this basin. This was out of the scope of this study because we here focused on a single case study considering one tsunamigenic zone (i.e., NAC) and one real tsunami event (i.e., the May 2003 tsunami). Nonetheless, this study has demonstrated that using a considerably less number of OBPGs compared to that of the S-net and DONET systems in Japan, TDA can produce reasonable tsunami forecasts to enhance the tsunami warning system in the WMB. We note that the sufficiency of a forecast accuracy for a particular region is usually decided by the Civil Protection Authorities (CPA) and warning center guidelines; this is normally a function of the characteristics of the tsunamigenic zones and their distances to population centers.

Conclusions

We conducted a case study of tsunami data assimilation (TDA) for the Western Mediterranean Basin (WMB) considering one of the tsunamigenic zones in this basin namely the North African Coast (NAC) and a real tsunami event in this zone (i.e., the May 2003 event). The objective of this research was to study whether deployment of offshore bottom pressure gauges (OBPGs) combined with TDA could be satisfactorily applied for tsunami warning system in the WMB. Four scenarios of OBPG arrangements involving 10, 5, 3 and 2 gauges were considered with distances of 120–300 km from the NAC. An assimilation window time of 20 min, from the earthquake origin time, was considered. Results showed that all four scenarios satisfactorily forecasted the May 2003 tsunami with forecast accuracies in the range of 69–85% and allowing warning lead times of

20, 30, 48 and 55 min for Ibiza, Palma, Sant Antoni and Barcelona, respectively. We conclude that deployment of OBPGs is beneficial for the tsunami warning system in the WMB. We note that our proposed OBPG arrangements are applicable only for the case of the May 2003 tsunami in the NAC. Detailed sensitivity analyses are required to propose OBPG designs that could be useful for various earthquake scenarios in the WMB.

Abbreviations

WMB: Western Mediterranean Basin; OBPGs: offshore bottom pressure gauges; TDA: tsunami data assimilation; CoS: coast of Spain; NAC: North African Coast; LS: Ligurian Sea; WCITS: west coast of Italy and Tyrrhenian Sea; NEAMTWS: North East Atlantic, Mediterranean and Connected seas Tsunami Warning System; ICG/NEAMTWS: Intergovernmental Coordination Group for the Tsunami Early Warning and Mitigation System in the North-eastern Atlantic; INGV: Istituto Nazionale di Geofisica e Vulcanologia (Italy); KOERI: Kandilli Observatory and Earthquake Research Institute (Turkey); NOA: National Observatory of Athens (Greece); TSPs: Tsunami Service Providers; DART: Deep-Ocean Assessment and Reporting of Tsunamis; S-net: Seafloor Observation Network for Earthquakes and Tsunamis; DONET: Dense Ocean-floor Network System for Earthquakes and Tsunamis; TTT: tsunami travel time; TUNAMI: Tohoku University's Numerical Analysis Model for Investigation of Near-field tsunamis.

Acknowledgements

The tsunami observation records, used in this study, are provided by UNESCO/IOC (Intergovernmental Oceanographic Commission), Puertos del Estado (Spain) (<http://www.puertos.es/>) and the European Sea Level Service (https://www.bodc.ac.uk/projects/data_management/european/eseas/). The authors would also like to thank these organizations for making the data available to us. The GMT (Generic Mapping Tool) software (Wessel and Smith 1998) was used for drafting most of the figures.

Authors' contributions

MH initiated the idea of this research and prepared the initial draft, conducted forward tsunami simulations and produced relevant figures and texts. YW conducted the tsunami data assimilations (TDA), wrote the data and methods relevant to TDA, produced figures relevant to TDA and contributed to "Results" and "Conclusions". KS provided critical insights on the performance of TDA in the Mediterranean Sea, contributed to the structure of the article and wrote parts of "Results" and "Conclusions". IEM contributed to the TDA analysis, optimization of the locations of offshore gauges in the Mediterranean Sea and contributed to the write-up of the manuscript. All authors read and approved the final manuscript.

Funding

MH is funded by the Royal Society (Grant number CH/LR1\180173), the Japan Society for the Promotion of Science (JSPS) (Grant number JSPS/IP/19003), and The Great Britain Sasakawa Foundation (Grant number 5542). YW's work was supported by JSPS KAKENHI Grant number JP19J20293.

Availability of data and materials

The sea level data used in this study come from the UNESCO/IOC (Intergovernmental Oceanographic Commission: <http://www.ioc-sealevelmonitoring.org>), the European Sea Level Service (<http://www.eseas.org>), and Puertos del Estado (Spain) (<http://www.puertos.es/>). The data are available in the aforesaid websites.

Competing interests

The authors declare that they have no competing interests.

Author details

¹ Department of Civil & Environmental Engineering, Brunel University London, Uxbridge UB8 3PH, UK. ² Earthquake Research Institute, The University of Tokyo, Tokyo 113-0032, Japan.

Author Proof

394
395
396
397
398
399
400
401
402
403
404
405
406
407
408
409
410
411
412
413
414
415
416
417
418
419
420
421
422
423
424
425
426
427
428
429
430
431
432
433
434
435
436
437
438
439
440
441
442
443
444
445
446
447
448
449
450
451
452
453

454 Received: 16 September 2019 Accepted: 3 December 2019
 455

References

456 Alasset PJ, Hébert H, Maouche S, Calbini V, Meghraoui M (2006) The tsunami
 457 induced by the 2003 Zemmouri earthquake (Mw = 6.9, Algeria): model-
 458 ling and results. *Geophys J Int* 166:213–226
 459 Déverchère J, Yelles K, Domzig A, Mercier de Lépinay B, Bouillin JP, Gaullier V,
 460 Bracène R, Calais E, Savoye B, Kherroubi A, Le Roy P (2005) Active thrust
 461 faulting offshore Boumerdes, Algeria, and its relations to the 2003 Mw 6.9
 462 earthquake. *Geophys Res Lett* 32:4
 463 Dogan GG, Annunziato A, Papadopoulos GA, Guler HG, Yalciner AC, Cakir
 464 TE, Sozdinler CO, Ulutas E, Arikawa T, Suzen ML, Guler I (2019) The
 465 20th July 2017 Bodrum-Kos tsunami field survey. *Pure Appl Geophys*
 466 176:2925–2949
 467 Eva C, Rabinovich AB (1997) The February 23, 1887 tsunami recorded
 468 on the Ligurian coast, western Mediterranean. *Geophys Res Lett*
 469 24(17):2211–2214
 470 Geoware (2011) The tsunami travel times (TTT). <http://www.geoware-online.com/tsunami.html>. Accessed Dec 2013
 471 Gonzalez FI, Milburn HM, Bernard EN, Newman JC (1998) Deep-ocean assess-
 472 ment and reporting of tsunamis (DART®): brief overview and status
 473 report. In: Proceedings of the international workshop on tsunami disaster
 474 mitigation, Tokyo, Japan, 19–22 January 1998
 475 Goto C, Ogawa Y, Shuto N, Imamura F (1997) Numerical method of tsunami
 476 simulation with the leap-frog scheme (IUGG/IOC Time Project). IOC
 477 Manual, UNESCO, No 35
 478 Gusman AR, Sheehan AF, Satake K, Heidarzadeh M, Mulia IE, Maeda T
 479 (2016) Tsunami data assimilation of Cascadia seafloor pressure gauge
 480 records from the 2012 Haida Gwaii earthquake. *Geophys Res Lett*
 481 43(9):4189–4196
 482 Heidarzadeh M, Gusman AR (2018) Application of dense offshore tsunami
 483 observations from Ocean Bottom Pressure Gauges (OBPGs) for tsunami
 484 research and early warnings. In: Durrani TS, Wang W, Forbes SM (eds) Geo-
 485 logical disaster monitoring based on sensor networks. Springer, Berlin, pp
 486 7–22. https://doi.org/10.1007/978-981-13-0992-2_2
 487 Heidarzadeh M, Satake K (2013) The 21 May 2003 tsunami in the Western
 488 Mediterranean Sea: statistical and wavelet analyses. *Pure Appl Geophys*
 489 170(9):1449–1462
 490 Heidarzadeh M, Satake K, Murotani S, Gusman AR, Watada S (2015) Deep-
 491 water characteristics of the trans-pacific Tsunami from the 1 April 2014 M
 492 w 8.2 Iquique, Chile Earthquake. *Pure Appl Geophys* 172(3):719–730
 493 Heidarzadeh M, Harada T, Satake K, Ishibe T, Gusman AR (2016) Comparative
 494 study of two tsunamigenic earthquakes in the Solomon Islands: 2015 Mw
 495 7.0 normal-fault and 2013 Santa Cruz Mw 8.0 megathrust earthquakes.
 496 *Geophys Res Lett* 43(9):4340–4349
 497 Heidarzadeh M, Necmioglu O, Ishibe T, Yalciner AC (2017) Bodrum–Kos (Tur-
 498 key–Greece) Mw 6.6 earthquake and tsunami of 20 July 2017: a test for
 499 the Mediterranean tsunami warning system. *Geosci Lett* 4:31
 500 IOC (Intergovernmental Oceanographic Commission, UNESCO) (2015)
 501 10 years of the North-Eastern Atlantic, the Mediterranean and Connected
 502 Seas Tsunami Warning and Mitigation System (NEAMTWS): accomplish-
 503 ments and challenges in preparing for the next tsunami. 59 pages. <https://unesdoc.unesco.org/ark:/48223/pf0000247393>
 504 Kalnay E (2003) Atmospheric modeling, data assimilation and predictability.
 505 Cambridge University Press, Cambridge
 506 Kanazawa T (2013) Japan trench earthquake and tsunami monitoring network
 507 of cable-linked 150 ocean bottom observatories and its impact to Earth
 508 disaster science. In: Underwater technology symposium (UT), 2013 IEEE
 509 international. Tokyo: IEEE; pp 1–5. <https://doi.org/10.1109/UT.2013.6519911>
 510 Kameda Y, Hirahara K, Furumura T (2009) New research project for evaluating
 511 seismic linkage around the Nankai trough-integration of observation,
 512 simulation, and disaster mitigation. *J Disaster Res* 4(2):61–66
 513 Kameda Y, Kawaguchi K, Araki E, Matsumoto H, Nakamura T, Kamiya S, Ariyoshi
 514 K, Hori T, Baba T, Takahashi N (2015) Development and application of an
 515 advanced ocean floor network system for megathrust earthquakes and
 516 tsunamis. In: Favali P, Beranzoli L, De Santis A (eds) Seafloor observatories.

Springer, Berlin, pp 643–662. https://doi.org/10.1007/978-3-642-11374-1_25
 521 Larroque C, Scotti O, Ioualalen M (2012) Reappraisal of the 1887 Ligurian earth-
 522 quake (western Mediterranean) from macroseismicity, active tectonics
 523 and tsunami modelling. *Geophys J Int* 190(1):87–104
 524 Maeda T, Obara K, Shinohara M, Kanazawa T, Uehira K (2015) Successive esti-
 525 mation of a tsunami wavefield without earthquake source data: a data
 526 assimilation approach toward real-time tsunami forecasting. *Geophys Res
 527 Lett* 42(19):7923–7932
 528 Meghraoui M, Maouche S, Chemaia B, Cakir Z, Aoudia A, Harbi A, Alasset PJ,
 529 Ayadi A, Bouhadad Y, Benhamouda F (2004) Coastal uplift and thrust
 530 faulting associated with the Mw = 6.8 Zemmouri (Algeria) earthquake of
 531 21 May, 2003. *Geophys Res Lett* 31(19)
 532 Mulia IE, Gusman AR, Satake K (2017) Optimal design for placements of
 533 tsunami observing systems to accurately characterize the inducing
 534 earthquake. *Geophys Res Lett* 44:12106–12115
 535 Mulia IE, Gusman AR, Williamson AL, Satake K (2019) An optimized array con-
 536 figuration of tsunami observation network off Southern Java, Indonesia. *J
 537 Geophys Res.* <https://doi.org/10.1029/2019JB017600>
 538 Necmioğlu Ö (2016) Design and challenges for a tsunami early warning
 539 system in the Marmara Sea. *Earth Planets Space* 68:13
 540 Necmioğlu O, Özel NM (2015) Earthquake scenario-based tsunami wave
 541 heights in the Eastern Mediterranean and connected seas. *Pure Appl
 542 Geophys* 172(12):3617–3638
 543 Okada Y (1985) Surface deformation due to shear and tensile faults in a half-
 544 space. *Bull Seismol Soc Am* 75:1135–1154
 545 Okal EA, Synolakis CE, Uslu B, Kalligeris N, Voukouvalas E (2009) The 1956 earth-
 546 quake and tsunami in Amorgos, Greece. *Geophys J Int* 178(3):1533–1554
 547 Öztürk S, Şahin Ş (2019) A statistical space-time-magnitude analysis on the
 548 aftershocks occurrence of the July 21th, 2017 MW = 6.5 Bodrum–Kos,
 549 Turkey, earthquake. *J Asian Earth Sci* 172:443–457
 550 Papadopoulos GA (2015) Tsunami in the European-Mediterranean Region:
 551 from historical record to risk mitigation. Elsevier, Amsterdam, p 290. ISBN
 552 978-0-12-420224-5
 553 Papadopoulos GA, Fokaefs A (2013) Near-field tsunami early warning and
 554 emergency planning in the Mediterranean Sea. *Res Geophys* 3:24–31
 555 Rabinovich AB, Eblé MC (2015) Deep-ocean measurements of tsunami waves.
 556 *Pure Appl Geophys* 172:3281–3312
 557 Roger J, Hébert H (2008) The 1856 Djijelli (Algeria) earthquake and tsunami:
 558 source parameters and implications for tsunami hazard in the Balearic
 559 Islands. *Nat Hazards Earth Syst Sci* 8(4):721–731
 560 Sahal A, Roger J, Allgeyer S, Lemaire B, Hébert H, Schindelé F, Lavigne F (2009)
 561 The tsunami triggered by the 21 May 2003 Boumerdes–Zemmouri (Algeria)
 562 earthquake: field investigations on the French Mediterranean coast
 563 and tsunami modelling. *Nat Hazards Earth Syst Sci* 9(6):1823
 564 Satake K (2014) Advances in earthquake and tsunami sciences and disaster risk
 565 reduction since the 2004 Indian ocean tsunami. *Geosci Lett* 1(1):15
 566 Synolakis CE, Bernard EN (2006) Tsunami science before and beyond Boxing
 567 Day 2004. *Philos Trans R Soc Lond A* 364(1845):2231–2265
 568 Tinti S, Graziani L, Brizuela B, Maramai A, Gallazzi S (2012) Applicability of the
 569 decision matrix of North Eastern Atlantic, Mediterranean and connected
 570 seas Tsunami Warning System to the Italian tsunamis. *Nat Hazards Earth
 571 Syst Sci* 12:843–857
 572 Tsushima H, Hino R, Fujimoto H, Tanioka Y, Imamura F (2009) Near-field
 573 tsunami forecasting from cabled ocean bottom pressure data. *J Geophys
 574 Res Solid Earth* 114:B06309. <https://doi.org/10.1029/2008JB005988>
 575 Wang Y, Satake K, Maeda T, Gusman AR (2017) Green's function-based tsunami
 576 data assimilation: a fast data assimilation approach toward tsunami early
 577 warning. *Geophys Res Lett* 44(20):10–282
 578 Wang Y, Satake K, Maeda T, Gusman AR (2018) Data assimilation with disper-
 579 sive tsunami model: a test for the Nankai Trough. *Earth Planets Space*
 580 70(1):131
 581 Wang Y, Maeda T, Satake K, Heidarzadeh M, Su H, Sheehan AF, Gusman AR
 582 (2019) Tsunami data assimilation without a dense observation network.
 583 *Geophys Res Lett* 46(4):2045–2053
 584 Weatherall P, Marks KM, Jakobsson M, Schmitt T, Tani S, Arndt JE, Rovere M,
 585 Chayes D, Ferrini V, Wigley R (2015) A new digital bathymetric model of
 586 the world's oceans. *Earth Space Sci* 2:331–345
 587 Wessel P, Smith WHF (1998) New, improved version of generic mapping tools
 588 released. *EOS Trans AGU* 79(47):579
 589

Author Proof

518 AQ4
 519
 520

591 Yalçiner A, Pelinovsky E, Talipova T, Kurkin A, Kozelkov A, Zaitsev A (2004)
 592 Tsunamis in the Black Sea: comparison of the historical, instrumental, and
 593 numerical data. *J Geophys Res* 109(C12)
 594 Yamamoto N, Aoi S, Hirata K, Suzuki W, Kunugi T, Nakamura H (2016) Multi-
 595 index method using offshore ocean-bottom pressure data for real-time
 596 tsunami forecast. *Earth Planets Space* 68(1):128
 597 Yang Y, Dunham EM, Barnier G, Almquist M (2019) Tsunami wavefield recon-
 598 struction and forecasting using the ensemble Kalman Filter. *Geophys Res*
 599 *Lett* 46:853–860

Publisher’s Note

Springer Nature remains neutral with regard to jurisdictional claims in published maps and institutional affiliations.

600
 601
 602

Author Proof

UNCORRECTED PROOF

Submit your manuscript to a SpringerOpen® journal and benefit from:

- ▶ Convenient online submission
- ▶ Rigorous peer review
- ▶ Open access: articles freely available online
- ▶ High visibility within the field
- ▶ Retaining the copyright to your article

Submit your next manuscript at ▶ springeropen.com